



Farhan, Ahmed Hilal and Dawson, Andrew Robert and Thom, Nicholas Howard (2016) Characterization of rubberized cement bound aggregate mixtures using indirect tensile testing and fractal analysis. *Construction and Building Materials*, 105 . pp. 94-102. ISSN 0950-0618

**Access from the University of Nottingham repository:**

<http://eprints.nottingham.ac.uk/34784/1/Paper%20%20%20Characterization%20of%20rubberized%20cement%20bound%20aggregate%20mixtures%20using%20indirect%20tensile%20testing%20and%20fractal%20analysis.pdf>

**Copyright and reuse:**

The Nottingham ePrints service makes this work by researchers of the University of Nottingham available open access under the following conditions.

This article is made available under the Creative Commons Attribution Non-commercial No Derivatives licence and may be reused according to the conditions of the licence. For more details see: <http://creativecommons.org/licenses/by-nc-nd/2.5/>

**A note on versions:**

The version presented here may differ from the published version or from the version of record. If you wish to cite this item you are advised to consult the publisher's version. Please see the repository url above for details on accessing the published version and note that access may require a subscription.

For more information, please contact [eprints@nottingham.ac.uk](mailto:eprints@nottingham.ac.uk)

# Characterization of rubberized cement bound aggregate mixtures using indirect tensile testing and fractal analysis

Ahmed Hilal Farhan\*, Andrew Robert Dawson, Nicholas Howard Thom

**Accepted manuscript**

<http://dx.doi.org/10.1016/j.conbuildmat.2015.12.018>

0950-0618/ 2015 Elsevier Ltd. All rights reserved

Please cite this article in press as: A.H. Farhan et al., Characterization of rubberized cement bound aggregate mixtures using indirect tensile testing and fractal analysis, *Constr. Build. Mater.* (2015), <http://dx.doi.org/10.1016/j.conbuildmat.2015.12.018>

1 **Characterization of rubberized cement bound aggregate mixtures using**  
2 **indirect tensile testing and fractal analysis**

3

4 **Ahmed Hilal Farhan\*, Andrew Robert Dawson, Nicholas Howard Thom**

5 School of Civil Engineering, Faculty of Engineering, University of Nottingham, University Park,  
6 Nottingham NG7 2RD, UK, Tel: +44 (0) 7448461314, E-mail: evxahfa@nottingham.ac.uk

7 \*corresponding author

8

9

10 **Abstract**

11 The main focus of this paper is to investigate the tensile properties of virgin and rubberized  
12 cement bound granular mixtures. This was conducted using indirect tensile testing with lateral  
13 displacement measurements, nondestructive resonant frequency testing, X-ray CT and  
14 quantitative assessment for cracking pattern using fractal analysis. The investigated properties  
15 were density, compacity, indirect tensile strength (ITS), indirect tensile static modulus,  
16 toughness, dynamic modulus of elasticity, dynamic modulus of rigidity, dynamic poisson's  
17 ratio, fractal dimension and fracture energy. To keep the same aggregate packing, the natural  
18 aggregate was replaced by waste tyres' crumb rubber of similar gradation. Four volumetric  
19 replacement percentages (0%, 15%, 30% and 45%) of the 6 mm fraction size were utilized.  
20 This adjustment was observed to affect the material density not only due to the lower specific  
21 gravity, but because it also affects the compactibility of the mixture negatively due to the  
22 damping action of the rubber particles. In addition, strength was also affected detrimentally.  
23 However, material toughness was improved and stiffness was mitigated. The latter findings  
24 were supported by quantitative assessment of the cracking pattern which revealed more  
25 tortuosity and a higher fractal dimension as a result of rubber content increasing. A failure  
26 mechanism for this type of mixture was suggested and support by examining the internal  
27 structure of failed samples using X-ray CT. Overall, construction of cement-stabilized

28 aggregate base with a small percentage of added crumb rubber may ensure a more sustainable  
29 and environmental-friendly pavement material and, at the same time, improve the properties  
30 of stabilized layers. However, behaviour of these mixtures under cyclic loading and  
31 evaluation of their durability should be assessed to fully validate their use.

32

33 **Keywords:** cement-stabilized aggregate; waste tyres; rubberized cement bound mixture;  
34 indirect tensile; sustainable pavement; fractal analysis.

35

## 36 **1. Introduction**

37 Stockpiling waste materials and depletion of natural resources represent two accompanying  
38 problems in the modern world. One of the most common and continuously increasing waste  
39 materials is derived from the vehicle tires consumed every year. Over the years, many authors  
40 have attempted to make use of these waste materials to ensure proper disposal of these  
41 materials and to save natural resources. Authors (Khatib and Bayomy 1999; Güneyisi et al.  
42 2004; Papakonstantinou and Tobolski 2006; Balaha et al. 2007; Gesoğlu and Güneyisi 2007;  
43 Zheng et al. 2007; Khaloo et al. 2008; Taha et al. 2008; Zheng et al. 2008; Güneyisi 2010;  
44 Pelisser et al. 2011; Najim and Hall 2012; Güneyisi et al. 2014) have investigated the  
45 feasibility of using waste tire materials in different types of concrete mixtures as a  
46 replacement of either fine or coarse aggregate or both. Others (Pincus et al. 1994; Cecich et al.  
47 1996; Foose et al. 1996; Masad et al. 1996; Liu et al. 2000; Youwai and Bergado 2003; Kim  
48 et al. 2005; Humphrey 2007) studied the possible use of these materials in geotechnical  
49 applications as fill materials for embankments and behind retaining walls.

50

51 No doubt, highway construction consumes large quantities of natural materials as compared  
52 with other civil engineering projects (Cao 2007; Barišić et al. 2014). Therefore, studies have  
53 been conducted to investigate the possibility of using these waste materials within the  
54 pavement structure, specifically in asphaltic mixtures to modify the properties of the binder

55 either through the wet or dry process (Chiu and Lu 2007; Fontes et al. 2010); (Cao 2007; Xiao  
56 et al. 2007; Chiu 2008). A very few studies were conducted to investigate the possibility of  
57 using crumb rubber within cement-stabilized aggregate mixtures typically used as a base  
58 and/or subbase courses in flexible composite pavement structure. The usage in this case might  
59 be more feasible than in asphaltic mixtures used as a base or surface course since the latter  
60 two layers usually have a limited thickness due to their high cost as compared with cement-  
61 stabilized layers. Cement-stabilized mixtures as defined by (Lim and Zollinger 2003) are a  
62 mixture of aggregate, Portland cement and a small quantity of water to facilitate compaction  
63 and to hydrate the cement. Cement-stabilized aggregate can be classified as a cementitious  
64 material. The Portland Concrete Association (PCA 2005) has classified these materials into  
65 four types depending on the amount of water and cement being used. Materials with high  
66 cement contents are roller-compacted concrete and normal concrete. However, the first one is  
67 constructed by rolling due to the low level of water as compared with the latter. On the other  
68 hand, flowable fill and cement-stabilized materials are the other types which contain low  
69 cement levels with first one being constructed by rolling due to its low water content.

70  
71

## 72 **2. Rationale and aims**

73 The motivation of this research is to make use of the above waste materials which in turn  
74 should help to save natural resources as well as to reduce the environmentally detrimental  
75 effect of these materials. Another motivation comes from the fact that the use of Portland  
76 cement to stabilize granular materials usually produces stiff mixtures which are sensitive to  
77 cracking, overloading and fatigue failure (Wu et al. 2015). Furthermore, the reflection cracks  
78 mostly accompanying the cement-stabilization, especially at high cement contents.  
79 Consequently, an attempt was made in this paper to mitigate the above disadvantages by  
80 using the crumb rubber to modify some cement-stabilized mixtures. The purpose of this paper  
81 is to study the effect of crumb rubber particles on the properties of cement-stabilized mixtures,  
82 mainly in terms of tensile performance. The importance of this investigation comes from the

83 fact that, in pavement structural design, tensile properties are the most influential factors since  
84 all bound layers (including cement bound granular mixture (CBGM) are designed based on  
85 the tensile stress / strain at the bottom of these layers. A review of literature indicated that  
86 there is no published study about the quantitative evaluation of cracking pattern of rubberized,  
87 nor even of conventional cement-stabilized materials. Therefore, another complementary  
88 objective of this paper is to use the fractal analysis concept to quantitatively study the  
89 cracking pattern of cement-stabilized aggregate containing different rubber contents and to  
90 investigate any possible correlation with macro-scale properties. This will help to better  
91 understand the failure mechanism of this type of modified mixture.

92

### 93 **3. Experimental program and methodology**

#### 94 **3.1 Materials and their properties**

95 A crushed limestone aggregate of 20 mm maximum size is used across this study. To ensure  
96 the manufacture of comparable mixtures containing the same gradation and densities and  
97 hence investigating the effect of rubber alone, two steps were conducted. The first one was to  
98 use and combine different fractional sizes (20 mm, 14 mm, 10 mm, 6 mm and dust (less than  
99 6mm)) in different proportions to constitute the required gradation and the second was to  
100 batch, mix and compact each sample individually. This was so as to ensure comparable  
101 strength since there is a high dependency of the strength on mixture density (Williams 1986).  
102 Different fractions of limestone aggregate were collected from Dene Quarry in  
103 Nottinghamshire in the UK. The gradations were assessed in accordance with BS EN 933-  
104 1:2012. The crumb rubber particles were sourced from J Allcock and Sons Ltd. in  
105 Manchester, UK. Its gradation is presented in Figure 1. Initial examination showed a  
106 similarity between the 6 mm aggregate fraction size and that of crumb rubber as shown in this  
107 figure. Consequently, it was decided to replace the former by the latter in order to ensure the  
108 same aggregate packing so as to enable study of the effect of elastic aggregate particles alone.

109 The specific gravity of the rubber was adopted as 1.12 as measured by (Najim and Hall 2012).  
110 CEM I 52.5 R Portland cement conforming to BS EN 197-1: 2000 was used for aggregate  
111 mixtures stabilization. Potable tap water was utilized to moisturize the cement- aggregate  
112 mixture.

113

### 114 **3.2 Mixture design and samples production**

115 The final gradation, after blending, of the CBGM was to specification BS EN 14227-1:2013 -  
116 [CBGM2-0/20]. It is illustrated in Figure 2. 5% cement, by dry weight of aggregate, was used.  
117 Optimum water content for aggregate-cement mixture was estimated as 4.6% (by the total dry  
118 weight of aggregate and cement) in accordance with BS EN 13286-4:2003. Regarding the  
119 degree of replacement by rubber, three volumetric replacement percentages was investigated  
120 and the resulting materials compared with mixtures contain no rubber. These are 15%, 30%  
121 and 45% of the 6 mm aggregate fraction volume. These are equivalent to 2.1%, 4.2% and  
122 6.2% of the total volume of the aggregate, respectively. Because of the considerable  
123 differences between the specific gravities of natural aggregate and crumb rubber,  
124 proportioning on the weight basis is a misleading approach. This is because the cement is  
125 normally added by the dry weight of aggregate which will reduce after replacing with crumb  
126 rubber due to the low specific gravity of the latter. This in turn would cause a change in the  
127 cement content and accordingly water content for different replacement levels. Accordingly,  
128 volumetric proportioning was taken into consideration. All volumetric proportion was kept  
129 constant as used in the virgin mixture and the only variable was the rubber volume. This was  
130 simply done by keeping the weight of cement and water as that used in the virgin mix. For the  
131 purpose of designation, C5R0 was used to indicates the mixture containing 5% cement  
132 content and 0% rubber replacement i.e., virgin mix. On the other hand, C5R15, C5R30 and  
133 C5R45 were used to describe the mixtures containing 5% cement and 15, 30 and 45%  
134 replacement levels, respectively.

135

136 Regarding mixing sequence, cement and dust were mixed firstly until uniform colour was  
137 achieved. The cement- dust mixtures was added to the rest of aggregate sizes and mixed for a  
138 minute. After adding the appropriate water quantity, all materials were mixed thoroughly for  
139 another two minutes. All mixing was conducted manually. On completion of mixing, each  
140 mixture was compacted in three layers inside a lubricated spilt mould with diameter of 101.6  
141 mm using a Kango 638 vibrating hammer. The compaction time was 60 sec. per layer as  
142 recommended by BS EN 13286-51:2004. Past experience with testing cement-stabilized  
143 samples predicted that a very low strain would develop during testing and that there would be  
144 a high sensitivity to the small unevenness in the surface which the loading platens touch,  
145 necessitating accurate instrumentation (Scullion et al. 2008). From initial investigations made  
146 during this study, the impossibility of achieving a smooth and level surface, which will make  
147 it is difficult to fix the instrumentations, had been observed. To overcome this problem, it was  
148 decided to manufacture the sample to achieve a height of about 115 mm and then trim it down  
149 to 100 mm. In addition, another set of samples was manufactured for resonant frequency  
150 testing using standard split moulds of 150 mm diameter and 300 mm height. Again, a  
151 removable mould extension was fabricated and used to ensure a specimen more than 300 mm  
152 tall which was then sawn down to 300 mm using a diamond saw. Three samples were  
153 manufactured for each mix. Once the compaction was finished, specimens were left inside  
154 their moulds and covered with wet paper and polythene sheets overnight to prevent moisture  
155 loss. On the next day, these were demoulded and wrapped with nylon film and placed in wet  
156 polythene bags and closed tightly and left in a humid room for 28 days.

157

### 158 **3.3 Testing procedures and analysis performed**

#### 159 **3.3.1 Compacity and density**

160 It was observed that the performance of cement-stabilized aggregate mixture is greatly  
161 dependent on its density. (Williams 1986) has reported that a 5% reduction in mixture density



162 causes 40-50 % reduction in the mixture strength. Thus, effective compaction can be expected  
163 to be critical for adequate performance. Accordingly, the British specification (BS EN 14227-  
164 1:2013) has introduced the compacity factor as a measure of the efficiency of compaction. It  
165 has been reported by the above specification that the compacity for cement-bound mixtures  
166 should be not less than 0.82. Critical analysis of this criterion shows that this is a movement  
167 towards the concept applied in asphaltic mixture to calculate the percent of air-voids.  
168 Compacity can be calculated as [100 - % air-voids]. In the current paper, due to the damping  
169 tendency of the rubber particles, these may affect the effectiveness of compaction negatively.  
170 Therefore, an investigation was carried out to evaluate if the rubber particle have a  
171 detrimental effect on the compactibility of the mixtures. Compacity in accordance with the  
172 above specification can be calculated using the following equation

173

$$C = \left(\frac{\gamma_m}{100}\right) \times \left(\frac{a}{\gamma_A} + \frac{b}{\gamma_B} + \frac{c}{\gamma_C} \dots\right)$$

174 where: C is the compacity factor,  $\gamma_m$  is the maximum dry density of the mixture and  $\gamma_A$ ,  $\gamma_B$ ,  
175  $\gamma_C$ , are particle densities of material A, B and C, respectively. a, b, c represent the percentages  
176 of material A, B, C in the total mixture. Dry density of the specimens was measured after  
177 curing by drying them in an oven at  $105 \pm 5^\circ\text{C}$  until constant weight, then using the water  
178 displacement method to measure the density.

179

### 180 **3.3.2 Indirect tensile strength and static modulus of elasticity**

181 This test was performed at 28 days in accordance with BS EN 13286-42:2003. A 200 KN  
182 capacity Instron universal testing machine was used. The indirect tensile strength (ITS), in  
183 MPa, was estimated using the following equation:  $\text{ITS} = 2P/\pi hD$  where P is the ultimate load  
184 (N), h is the sample thickness (mm) and D is the diameter of the sample (mm). In order to  
185 estimate the static modulus of elasticity, deformation was measured utilizing two linear  
186 variable differential transducers (LVDTs) mounted using LVDTs' blocks. These were glued  
187 on the both faces of specimen. Figure 3 illustrates the indirect tensile testing configuration. To

188 ensure accurate instrumentation, the gluing jig was manufactured and used as reported by  
 189 (Wen et al. 2014) to ensure precise alignment of the LVDTs blocks on both faces of the  
 190 sample. The average displacement value from these two LVDTs was used at each load  
 191 application. Finally, the static elastic modulus was estimated for a load being 30% of the  
 192 maximum load, and the corresponding lateral displacement according to EN 13286-43:2003.  
 193 However, instead of using the equation provided in the latter specification, which assumes  
 194 specific arrangement for the LVDTs, the following formula was used (Solanki and Zaman  
 195 2013):

$$E = \frac{2P}{\pi \cdot D \cdot t \cdot \Delta H_T (D^2 + D_g^2)} \left\{ (3 + \nu) D^2 \cdot D_g + (1 - \nu) \left[ D_g^3 - 2D(D^2 + D_g^2) \tan^{-1} \left( \frac{D_g}{D} \right) \right] \right\}$$

197

198 Where: P= load; D=diameter of sample; t= sample thickness;  $\Delta H_T$ =lateral deformation;  
 199  $D_g$ =LVDTs gauge distance and  $\nu$  = Poisson's ratio.

200

### 201 3.3.3 Mesostructural investigation

202 To better understand the failure mechanism and to observe how the cracks propagated, failed  
 203 specimens were scanned using an X- ray CT machine. This includes two systems located in  
 204 the same cabinet. The first one is the mini focus system of a 300 kV X-ray source and a linear  
 205 detector. The second system is a micro focus having a 225 kV with an area detector. To  
 206 ensure sufficient power of X-ray for penetration through stabilized mixtures, the first system  
 207 was used in this investigation. Two scans were done for each sample at the top and bottom of  
 208 the middle third of sample. The resolution of the reported scan is 0.065 mm/pixel.

209

### 210 3.3.4 Toughness through indirect tensile test

211 To obtain the post-peak load-deflection behaviour and hence quantify toughness of the  
 212 material, the test was performed at a deformation rate of 0.5 mm/min. The corresponding

213 deflection was measured as mentioned earlier. To evaluate the post-peak loading bearing  
214 capacity enhancement, the area under the load-deformation curve can be used to compute the  
215 toughness or energy absorption capacity of the material. The estimation of toughness in this  
216 manner may include the improvement in strength and ductility due to rubber incorporation as  
217 stated by (Sobhan and Mashnad 2000). However, due to the reduction in the strength of the  
218 mixture as a result of rubber inclusion, it is necessary to normalize the load to its ultimate  
219 value to evaluate the enhancement in terms of ductility only. This is also logical since in the  
220 mechanistic pavement design the stress is usually normalized with respect to the strength and  
221 the stress ratio is normally used.

222

### 223 **3.3.5 Dynamic properties through resonant frequency**

224 Dynamic modulus of elasticity represents an important input for pavement analysis and  
225 design. (Nunn 2004) in TRL615 report and (Lav et al. 2006) adopted dynamic modulus as  
226 determined from resonant frequency for pavement design. In the present paper, dynamic  
227 properties were measured nondestructively using a resonant frequency tester (ERUDITE) in  
228 accordance with (ASTM C215-02). In this test, dynamic properties were evaluated in terms of  
229 dynamic modulus of elasticity ( $E_d$ ), dynamic modulus of rigidity ( $G_d$ ) and dynamic Poisson's  
230 ratio ( $\nu_d$ ). During the test, the sample was supported at its centre on the equipment bench and  
231 clamped in place. The driver and pick up parts were placed at different locations depending  
232 on whether dynamic modulus of elasticity or dynamic modulus of rigidity is to be measured.  
233 For each dynamic modulus type, there is a different recommended frequency range as shown  
234 in the equipment manual. Using the recommended frequency range and starting from a low  
235 frequency, the frequency was increased gradually until the output meter showed the maximum  
236 value which indicates the fundamental resonant frequency of the mixture. The latter was used  
237 to calculate the dynamic modulus of elasticity ( $E_d$ ) and dynamic shear modulus ( $G_d$ ) as  
238 explained in the above specification. From these two moduli, dynamic Poisson's ratio was  
239 estimated as  $\nu_d = (E_d/2G_d)$ .

### 240 3.3.6 Damage quantification using fractal analysis and image processing

241 To provide better a understanding of the mechanism of failure of this type of mixture, the  
242 failure cracking pattern was characterized quantitatively using fractal analysis. This technique  
243 has been extensively used in normal concrete to quantify cracking patterns (Erdem et al. 2012;  
244 Farhidzadeh et al. 2014) and fractured surfaces (Issa and Hammad 1994; Carpinteri et al.  
245 1999; Guo et al. 2007). However, no published study was found in literature regarding the  
246 quantification of surface cracks of cement-stabilized mixtures using fractal analysis. In this  
247 study, the fractal analysis was performed in terms of the fractal dimension. The latter was  
248 estimated using the box-counting method (Mihashi et al. 2006; Erdem and Blankson 2013).  
249 An initial investigation performed to extract topological information concerning the cracked  
250 area using image processing software, ImageJ, had difficulty in differentiating between the  
251 cracks and the rubber particles utilizing a grey thresholding process. For this reason it was  
252 decided to digitize the crack network using the following procedure: images of failed samples  
253 were firstly captured using a high resolution camera. These images were inserted into  
254 AutoCAD software and scaled up to reflect the actual dimensions. The cracks were digitized  
255 after that using the software tools. Then these were covered by imaginary meshes with  
256 rectangular grid sizes decreasing linearly (Figure 4). Then the number of grid squares required  
257 to cover the cracks was counted. Finally the fractal dimension was computed from the slope  
258 of the line joining the logarithm of number of grid squares encountered by the crack and the  
259 logarithm of the grid square dimension. From surface macro-crack fractal dimension, the  
260 fracture energy was roughly estimated based on the formula suggested by (Guo et al. 2007)  
261 which is  $W_s/G_f = a * (\delta/a)^{1-D_{1-d}}$  where  $W_s$  is the energy dissipated at the surface of the crack,  $G_f$   
262 is the fracture energy at the observation scale,  $a$  is the Euclidean length (equal to the diameter  
263 of the sample) and  $D_{1-d}$  is the fractal dimension computed previously.

264  
265  
266  
267  
268  
269

270 **4. Results and discussion**

271 **4.1 Density and compacity**

272 Table 1 shows a reduction in the material density after rubber incorporation. This is logical  
273 since the specific gravity of natural aggregate is much higher than that of crumb rubber.  
274 However, unlike natural aggregate, rubber particles of high elasticity may absorb the energy,  
275 due to their damping characteristics, from a vibrating hammer. This could causes a reduction  
276 in the compaction efficiency and, hence in mixture density. As can be seen from Table 1, the  
277 maximum difference was at a rubber replacement of 45% where there is a 0.92% reduction in  
278 the compacity of the mixture (i.e, a decline in density). This can lead to the conclusion that it  
279 is not only the low specific gravity of rubber that is responsible for density reduction, but it is  
280 also the reduction in compaction efficiency, due to the damping action of the rubber particles,  
281 that affects the density of the mixture detrimentally. The practical consequence of the latter  
282 finding is to avoid high levels rubber replacement in compacted mixtures.

283  
284

285 **4.2 Indirect tensile strength**

286 It is generally accepted that all cementitious materials (including concretes) are weak in  
287 tension and have low strain capacity. It was found that replacement of natural aggregate by  
288 crumb rubber has a negative effect on the indirect tensile strength (ITS) as shown in Figure 5.  
289 ITS decreased by 3% for each 1% of rubber replacement. This can be attributed, in addition to  
290 the lower modulus of elasticity, to the decrease in the number of contacts points between  
291 natural aggregate particles as a result of compacity drop and hence a reduction in the  
292 efficiency of aggregate interlock. This may affect the frictional resistance and accelerated  
293 mixture deterioration since frictional resistance is one of the main mechanisms for sustaining  
294 loads. The same decrease in ITS was observed at both 7 and 28 days for all mixes except  
295 C5R45 where there was no further reduction in this parameter, perhaps because of a specific  
296 rubber distribution.  
297

### 298 **4.3 load-deformation relationship, static modulus of elasticity and toughness**

299 The load-deformation relationships for different mixtures are illustrated in Figure 6. From  
300 these curves, toughness index was calculated as shown in Figure 7. It is clearly seen, at all  
301 replacement levels, that there was an improvement in the energy absorption capacity of the  
302 mixtures. This improvement was around about 27%. Although many researcher reported  
303 similar behaviour when they investigated the effect of rubber on toughness of normal concrete,  
304 no clear reasons was reported to explain this behaviour. However, (Chiaia et al. 1998)  
305 claimed that the ductility improvement when using weak aggregates is due to a change in the  
306 mechanism of microcracking. The reasons behind ductility improvement due to rubber  
307 addition in cement-stabilized materials might be a) partly because the crumb rubber particles  
308 helped to delay crack propagation by relieving some induced local stresses b) and partly due  
309 to embedding of weak particles inside stiff media lengthening the crack path since the crack  
310 path tends to propagate through these weak points. In addition, since the cracks tend to be  
311 propagating as a main crack and branches rather than one main crack, especially for rich  
312 rubber mixtures, this would cause more energy dissipation as described by Shah et al. (1995)  
313 and (Erdem 2012). To clarify the mechanism of failure and to elucidate the above hypotheses,  
314 X-ray CT was utilized to investigate the internal structure of failed samples at mesoscale level.  
315 Part (b) of the suggested mechanism is evidenced in Figure 8 which shows how the cracks  
316 propagated for different mixtures containing different rubber contents. Examining these scans  
317 clearly supports the suggested failure mechanism as the cracks can be seen to connect rubber  
318 particles as indicated by the red arrows in the same figure and tend to avoid areas without  
319 rubber (as predicted by reason (b) above). Furthermore, the load-deflection responses and  
320 estimated improved energy absorption capacity clearly support the explanation (a) of the  
321 mechanism suggested as presented in Figure 7. This was also supported by the tortuous and  
322 complex crack pattern as highlighted in fractal analysis. No doubt the applicability of this  
323 proposed mechanism depends, to some extent, on the distribution of the rubber particles. The

324 more uniform the rubber distribution, the more uniform the stress/strain distribution can be  
325 anticipated inside the mixture.

326

327 As the stiffness of the mixture depends, to a large extent, on the stiffnesses of its constituents,  
328 replacement of stiffer natural aggregate by softer crumb rubber particles reduces the stiffness  
329 of the mixture as shown in Figure 9. The increase in the stiffness of C5R45 relative to C5R30  
330 might be because of the less uniform distribution of rubber particles in the mixture. Perhaps  
331 an accumulation of rubber particles caused a stress concentration and resulted in premature  
332 failure of the sample without large deformation.

333

334

#### 335 **4.4 Dynamic properties**

336 Similar to the static modulus of elasticity results, there was a decrease in both dynamic  
337 modulus of elasticity and that of rigidity due to rubber replacement, as shown in Figure 10.  
338 This is because these two moduli depend on mixture density and type of aggregate. However,  
339 these parameters decreased linearly at all replacement levels. This, in fact, supports the above  
340 hypothesis regarding the possible rubber accumulation. As it known, during nondestructive  
341 testing, there was zero applied stress which eliminates the formation of micro-cracks and  
342 possible creep (Najim and Hall 2012). In other words, it depends on the mixture constituents  
343 and mixture fabrication alone. For this reason, it can be concluded that nondestructive testing  
344 does not depend, to a large extent, on rubber distribution as compared with sensitivity of  
345 destructive ones. With regard to dynamic Poisson's ratio, Figure 11 shows a decline in the  
346 value of this parameter as rubber content increase in the mixture. This is consistent with  
347 Goulias and Ali (1997) as cited by (Nehdi and Khan 2001)

348

349

#### 350 **4.5 Damage quantification**

351 Figure 12 demonstrates the fractal dimensions and fracture energies for different rubber  
352 replacement levels. Generally, higher fractal dimensionality and fracture energy are observed  
353 as rubber replacement level increases. This means that as rubber content increases, more

354 energy will dissipate to fracture the sample as suggested by (Guo et al. 2007) and (Erdem  
355 2012). The possible explanation for this phenomenon is that when the cracks developed they  
356 propagated through the weak points (i.e., rubber particles), as noted previously. Before their  
357 propagation, the rubber particles tend to absorb energy developed at the crack tip when the tip  
358 reaches them, especially at the microcracking level. In addition, more energy will disperse  
359 since the cracks more easily propagate as branches rather than as one main crack, which  
360 agrees with (Yan et al. 2003) who attributed this to the disordered crack growth characteristics  
361 found in a mixture's internal structure during load application. This means that more energy  
362 was absorbed by the mixture before failure. Energy dissipation capacity improvement is one  
363 of the findings reported by (Atahan and Yücel 2012) when they investigated the effect of  
364 rubber on fracture energy of normal concrete during impact tests. The dissipated energy at the  
365 surface macro-crack based on fractal analysis correlated well (Figure 13) with the toughness  
366 of mixture calculated from the load-deformation responses. This supports the above  
367 explanation and confirms that a strong relationship exists between the cracking pattern,  
368 represented by the fractal dimension, and the toughness, a finding which is consistent with  
369 (Yan et al. 2002; Tang and Wang 2012).

370

## 371 **5. Conclusions**

372 The effect of replacement of natural aggregate by crumb rubber on the tensile properties and  
373 mechanism of their failure was investigated in this paper. This was done utilizing indirect  
374 tensile tests and fractal analysis. The following conclusions can be drawn:

375

- 376 1. Even though the reduction in density after replacement with crumb rubber is a logical  
377 finding due to the low specific gravity of rubber particles as compared with natural  
378 aggregate, this is not the only reason for density reduction. Evaluation of the  
379 compacity for different replacement levels revealed a decline in the effectiveness of



380 compaction as the rubber inclusion rate increased. This can be attributed to the  
381 damping effect that the rubber particles of high elasticity possess which may absorb  
382 some of the compaction energy during vibratory compaction.

383

384 2. Indirect tensile strength reduced due to the inclusion of rubber particles in cement-  
385 stabilized aggregates mixtures due to the weakness of these introduced particles.  
386 However, an increase was observed in the post-peak behaviour which caused an  
387 improvement in the toughness of the modified mixtures. In addition, the high stiffness  
388 of the original mixtures was mitigated after partial replacement with rubber particles.

389

390 3. By observing stress-strain responses and the failure pattern and examining the internal  
391 structure of the failed specimens, the failure mechanism for a rubberized compacted  
392 system has been proposed in this paper. It assumes that the crack propagates through  
393 rubber particles which are thought to be absorbing energy on the crack tip. In addition,  
394 due to the distribution of these weak particles, this may also lengthen the path of the  
395 crack. Both of these would improve the energy absorption capacity of the modified  
396 mixtures.

397

398 4. The Fractal analysis concept is found to permit quantitative distinguishing between  
399 different failure patterns of CBGMs. Findings indicate that there is an increasing  
400 fractal dimension due to rubber replacement. This also provides a support for the  
401 suggested failure mechanism.

402

403 5. Non-destructive investigation confirmed that added rubber produced less stiff  
404 materials. It is also proved the ability of this test method to distinguish between  
405 mixtures with low rubber contents and its suitability to assess the performance of these  
406 modified mixtures.

407

408 6. It is not recommended to use high content of rubber particles contents due to their  
409 negative effect on compactibility of the mixture and, accordingly, the strength of the

410 modified mixture. Evaluation of the durability of these mixtures and assessment of  
411 their performance under cyclic load is important to validate their use.

412

413

414

415

#### 416 **Acknowledgements**

417 The support from the Higher Committee of Education Development in Iraq (HCED) by  
418 providing a scholarship for this research is gratefully acknowledged. Thanks are also due to  
419 Dr. Luis Neves for his valuable discussion. Acknowledgement is also extended to Mr. Chris  
420 Fox for helping to perform the x-ray CT scans.

421

422

423

424

425

426

427

428

429

430

431

432 **Figure Captions**

433 Fig.1. Grain size distribution rubber and 6 mm natural aggregate.

434 Fig.2. Grain size distribution for investigated material (specification limit as defined by BS  
435 EN 14227-1:2013).

436 Fig.3. Indirect tensile testing configuration.

437 Fig.4. Methodology of fractal dimension calculation.

438 Fig.5. Indirect tensile strength for examined mixtures.

439 Fig.6. Load-diametrical deformation curves for different replacement levels: a. C5R0;  
440 b. C5R15; c. C5R30; and d. C5R45.

441 Fig.7. Effect of replacement on toughness indices.

442 Fig.8. Sample scans of the failed specimens showing crack propagation through rubber  
443 particles: A and B represents the mixtures with 30% and 45% rubber replacement,  
444 respectively.

445 Fig.9. Effect of rubber content on static modulus of elasticity.

446 Fig.10. Effect of rubber replacement on dynamic elasticity and shear moduli.

447 Fig.11. Effect of rubber replacement on dynamic Poisson's ratio.

448 Fig.12. Fractal dimensions for virgin and modified mixtures with different replacement level.

449 Fig.13. Correlation between mechanical and fractal analysis results.

450  
451  
452  
453  
454  
455  
456  
457  
458  
459  
460  
461  
462  
463  
464  
465  
466  
467  
468  
469  
470  
471  
472  
473  
474  
475  
476  
477  
478  
479

Table 1: Investigated mixtures, compacity and dry density

Mixture symbol	Compacity factor	Dry density, Kg/m <sup>3</sup>	COV, %
C5R0	0.9198	2421.79	0.5
C5R15	0.9189	2395.21	0.65
C5R30	0.9165	2364.96	1.4
C5R45	0.9114	2327.70	0.8

480  
481  
482  
483  
484  
485  
486  
487  
488  
489  
490  
491  
492  
493  
494  
495  
496  
497  
498  
499  
500  
501  
502  
503  
504  
505  
506  
507  
508  
509

Table 2: Fractal analysis result summary

Mix ID	Fractal dimension	$W_s/G_f$
C5R0	1.013	103.99
C5R15	1.166	164.40
C5R30	1.219	192.70
C5R45	1.214	189.67

510 **References**

- 511 ASTM (C215-02). Standard Test Method for Fundamental Transverse, Longitudinal, and  
512 Torsional Frequencies of Concrete Specimens, ASTM International, West  
513 Conshohocken, PA, 2002, [www.astm.org](http://www.astm.org).
- 514 Atahan, A. O. and A. Ö. Yücel (2012). "Crumb rubber in concrete: Static and dynamic  
515 evaluation." Construction and Building Materials **36**: 617-622.
- 516 Balaha, M. M., A. A. M. Badawy and M. Hashish (2007). "effect of using ground waste tire  
517 rubber on the behavior of concrete mixes." Indian journal of Engineering and  
518 Materials Science **14**: 427-435.
- 519 Barišić, I., S. Dimter and T. Rukavina (2014). "Strength properties of steel slag stabilized  
520 mixes." Composites Part B: Engineering **58**: 386-391.
- 521 Cao, W. (2007). "Study on properties of recycled tire rubber modified asphalt mixtures  
522 using dry process." Construction and Building Materials **21**(5): 1011-1015.
- 523 Carpinteri, A., B. Chiaia and S. Invernizzi (1999). "Three-dimensional fractal analysis of  
524 concrete fracture at the meso-level." Theoretical and Applied Fracture Mechanics  
525 **31**(3): 163-172.
- 526 Cecich, V., L. Gonzales, A. Høisaeter, J. Williams and K. Reddy (1996). "Use of shredded  
527 tires as lightweight backfill material for retaining structures." Waste Management  
528 & Research **14**(5): 433-451.
- 529 Chiaia, B., J. Van Mier and A. Vervuurt (1998). "Crack growth mechanisms in four  
530 different concretes: microscopic observations and fractal analysis." Cement and  
531 Concrete Research **28**(1): 103-114.
- 532 Chiu, C.-T. (2008). "Use of ground tire rubber in asphalt pavements: Field trial and  
533 evaluation in Taiwan." Resources, conservation and recycling **52**(3): 522-532.
- 534 Chiu, C.-T. and L.-C. Lu (2007). "A laboratory study on stone matrix asphalt using  
535 ground tire rubber." Construction and Building Materials **21**(5): 1027-1033.
- 536 Erdem, S. (2012). Impact load-induced microstructural damage of concrete made with  
537 unconventional aggregates. PhD thesis, University of Nottingham.
- 538 Erdem, S. and M. A. Blankson (2013). "Fractal-fracture analysis and characterization of  
539 impact-fractured surfaces in different types of concrete using digital image  
540 analysis and 3D nanomap laser profilometry." Construction and Building  
541 Materials **40**: 70-76.
- 542 Erdem, S., A. R. Dawson and N. H. Thom (2012). "Impact load-induced micro-structural  
543 damage and micro-structure associated mechanical response of concrete made  
544 with different surface roughness and porosity aggregates." Cement and Concrete  
545 Research **42**(2): 291-305.
- 546 Farhidzadeh, A., E. Dehghan-Niri and S. Salamone (2014). "Crack pattern quantification  
547 of concrete structures based on fractal analysis." Safety, Reliability, Risk and Life-  
548 Cycle Performance of Structures and Infrastructures: 361.
- 549 Fontes, L. P., G. Trichês, J. C. Pais and P. A. Pereira (2010). "Evaluating permanent  
550 deformation in asphalt rubber mixtures." Construction and Building Materials  
551 **24**(7): 1193-1200.
- 552 Foose, G. J., C. H. Benson and P. J. Bosscher (1996). "Sand reinforced with shredded  
553 waste tires." Journal of Geotechnical Engineering **122**(9): 760-767.
- 554 Gesoğlu, M. and E. Güneyisi (2007). "Strength development and chloride penetration in  
555 rubberized concretes with and without silica fume." Materials and Structures  
556 **40**(9): 953-964.
- 557 Güneyisi, E. (2010). "Fresh properties of self-compacting rubberized concrete  
558 incorporated with fly ash." Materials and Structures **43**(8): 1037-1048.
- 559 Güneyisi, E., M. Gesoğlu, K. Mermerdaş and S. İpek (2014). "Experimental investigation  
560 on durability performance of rubberized concrete."
- 561 Güneyisi, E., M. Gesoğlu and T. Özturan (2004). "Properties of rubberized concretes  
562 containing silica fume." Cement and Concrete Research **34**(12): 2309-2317.
- 563 Guo, L.-P., W. Sun, K.-R. Zheng, H.-J. Chen and B. Liu (2007). "Study on the flexural  
564 fatigue performance and fractal mechanism of concrete with high proportions of  
565 ground granulated blast-furnace slag." Cement and Concrete Research **37**(2):  
566 242-250.

- 567 Humphrey, D. (2007). Tire derived aggregate as lightweight fill for embankments and  
568 retaining walls. Proceedings International Workshop on Scrap Tire Derived  
569 Geomaterials, Yokosuka, Japan.
- 570 Issa, M. and A. Hammad (1994). "Assessment and evaluation of fractal dimension of  
571 concrete fracture surface digitized images." Cement and Concrete Research **24**(2):  
572 325-334.
- 573 Khaloo, A. R., M. Dehestani and P. Rahmatabadi (2008). "Mechanical properties of  
574 concrete containing a high volume of tire-rubber particles." Waste Management  
575 **28**(12): 2472-2482.
- 576 Khatib, Z. K. and F. M. Bayomy (1999). "Rubberized Portland cement concrete." Journals  
577 of Materials in Civil Engineering, ASCE **11**: 206-213.
- 578 Kim, B., M. Prezzi and R. Salgado (2005). "Geotechnical properties of fly and bottom ash  
579 mixtures for use in highway embankments." Journal of geotechnical and  
580 geoenvironmental engineering **131**(7): 914-924.
- 581 Lav, A. H., M. A. Lav and A. B. Goktepe (2006). "Analysis and design of a stabilized fly  
582 ash as pavement base material." Fuel **85**(16): 2359-2370.
- 583 Lim, S. and D. G. Zollinger (2003). "Estimation of the compressive strength and modulus  
584 of elasticity of cement-treated aggregate base materials." Transportation  
585 Research Record: Journal of the Transportation Research Board **1837**(1): 30-38.
- 586 Liu, H., J. Mead and R. Stacer (2000). "Environmental effects of recycled rubber in light-  
587 fill applications." Rubber chemistry and technology **73**(3): 551-564.
- 588 Masad, E., R. Taha, C. Ho and T. Papagiannakis (1996). "Engineering properties of  
589 tire/soil mixtures as a lightweight fill material." Geotechnical Testing Journal(19).
- 590 Mihashi, H., S. Ahmed, T. Mizukami and T. Nishiwaki (2006). "Quantification of crack  
591 formation using image analysis and its relationship with permeability."
- 592 Najim, K. B. and M. R. Hall (2012). "Mechanical and dynamic properties of self-  
593 compacting crumb rubber modified concrete." Construction and Building Materials  
594 **27**(1): 521-530.
- 595 Nehdi, M. and A. Khan (2001). "Cementitious composites containing recycled tire rubber:  
596 an overview of engineering properties and potential applications." Cement  
597 Concrete and Aggregates **23**(1): 3-10.
- 598 Nunn, M. (2004). Development of a more versatile approach to flexible and flexible  
599 composite pavement design : prepared for highways agency, TRL report.
- 600 Papakonstantinou, C. G. and M. J. Tobolski (2006). "Use of waste tire steel beads in  
601 Portland cement concrete." Cement and Concrete Research **36**(9): 1686-1691.
- 602 PCA (2005). "soil cement technology for pavement different products for different  
603 applications." Portland Concrete Association(illinois).
- 604 Pelisser, F., N. Zavarise, T. A. Longo and A. M. Bernardin (2011). "Concrete made with  
605 recycled tire rubber: Effect of alkaline activation and silica fume addition." Journal  
606 of Cleaner Production **19**(6-7): 757-763.
- 607 Pincus, H., T. Edil and P. Bosscher (1994). "Engineering properties of tire chips and soil  
608 mixtures."
- 609 Scullion, T., J. Uzan, S. Hilbrich and P. Chen (2008). "Thickness Design Systems for  
610 Pavements Containing Soil-Cement Bases." PCA R&D Serial(2863).
- 611 Sobhan, K. and M. Mashnad (2000). "Fatigue durability of stabilized recycled aggregate  
612 base course containing fly ash and waste-plastic strip reinforcement." Final Rep.  
613 Submitted to the Recycled Materials Resource Centre, Univ. of New Hampshire.
- 614 Solanki, P. and M. Zaman (2013). "Behavior of Stabilized Subgrade Soils under Indirect  
615 Tension and Flexure." Journal of Materials in Civil Engineering **26**(5): 833-844.
- 616 Taha, M. M. R., A. S. El-Dieb, M. A. Abd El-Wahab and M. E. Abdel-Hameed (2008).  
617 "Mechanical, Fracture, and Microstructural Investigations of Rubber Concrete."  
618 Journal of Materials in Civil Engineering, ASCE **20**: 640-649.
- 619 Tang, W. and Y. Wang (2012). "Fractal characterization of impact fracture surface of  
620 steel." Applied Surface Science **258**(10): 4777-4781.
- 621 Wen, H., B. Muhunthan, J. Wang, X. Li, T. Edil and J. M. Tinjum (2014). Characterization  
622 of Cementitiously Stabilized Layers for Use in Pavement Design and Analysis.
- 623 Williams, R. I. T. (1986). "Cement-treated pavements : materials, design and  
624 construction " Elsevier Applied Science.

625 Wu, P., L. Houben, A. Scarpas, C. Egyed and R. de La Roij (2015). "Stiffness modulus  
626 and fatigue peoperties of cement-stabil;ized sand with use of a synthetic  
627 modified-zeolite additive." 2015 Annual meeting of transportation research board.  
628 Xiao, F., S. Amirkhanian and C. H. Juang (2007). "Rutting resistance of rubberized  
629 asphalt concrete pavements containing reclaimed asphalt pavement mixtures."  
630 Journal of Materials in Civil Engineering **19**(6): 475-483.  
631 Yan, A., K.-R. Wu, D. Zhang and W. Yao (2003). "Influence of concrete composition on  
632 the characterization of fracture surface." Cement and Concrete Composites **25**(1):  
633 153-157.  
634 Yan, A., K. Wu and X. Zhang (2002). "A quantitative study on the surface crack pattern  
635 of concrete with high content of steel fiber." Cement and Concrete Research **32**(9):  
636 1371-1375.  
637 Youwaj, S. and D. T. Bergado (2003). "Strength and deformation characteristics of  
638 shredded rubber tire sand mixtures." Canadian Geotechnical Journal **40**(2): 254-  
639 264.  
640 Zheng, L., X. Sharon Huo and Y. Yuan (2007). "Experimental investigation on dynamic  
641 properties of rubberized concrete." Construction and Building Materials **22**(5):  
642 939-947.  
643 Zheng, L., X. Sharon Huo and Y. Yuan (2008). "Strength, Modulus of Elasticity, and  
644 Brittleness Index of Rubberized Concrete." Journal of Civil Engineering , ASCE.

645

646



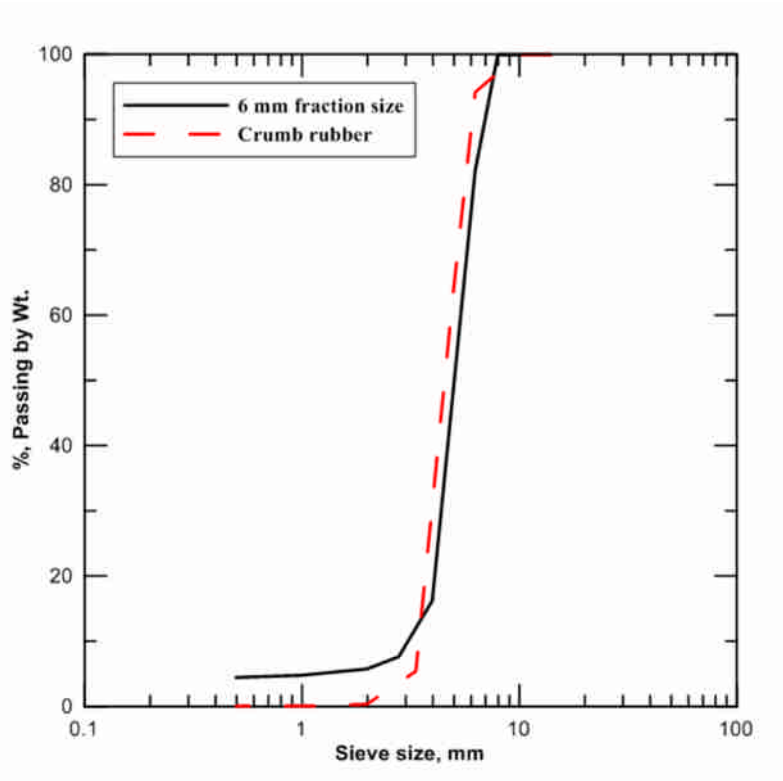


Figure 1: Grain size distribution rubber and 6 mm natural aggregate

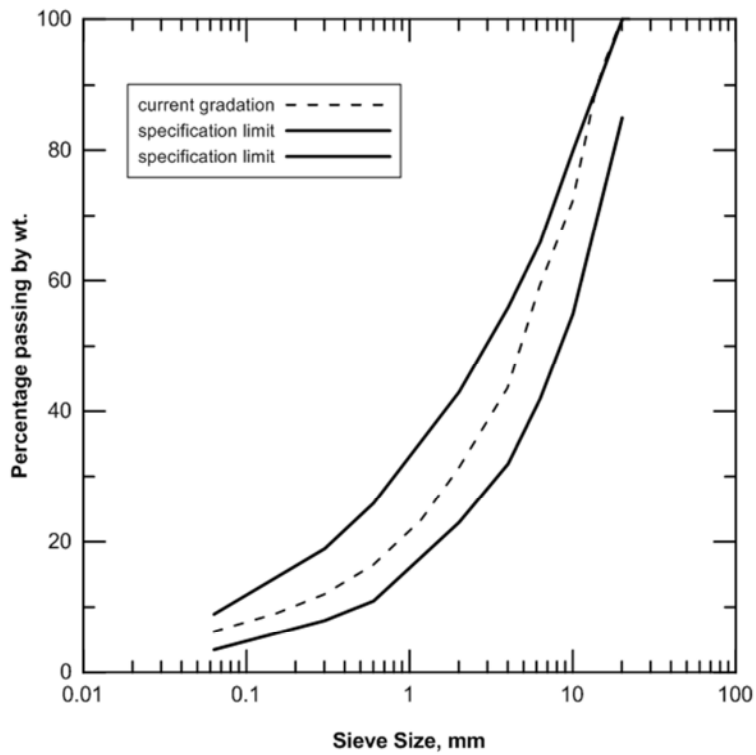


Figure 2: Grain size distribution for investigated material (specification limit as defined by BS EN 14227-1:2013)

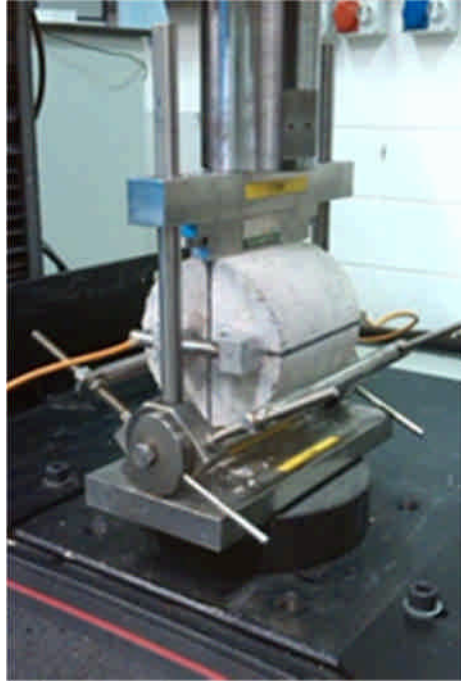


Figure 3: Indirect tensile testing configuration

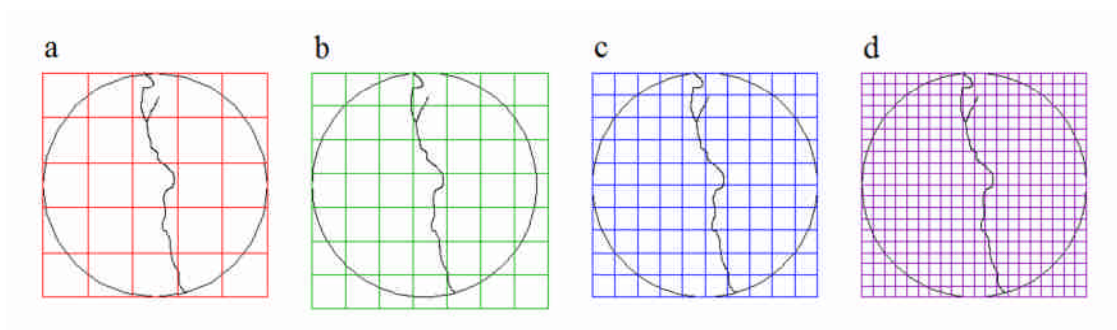


Figure 4: Methodology of fractal dimension calculation

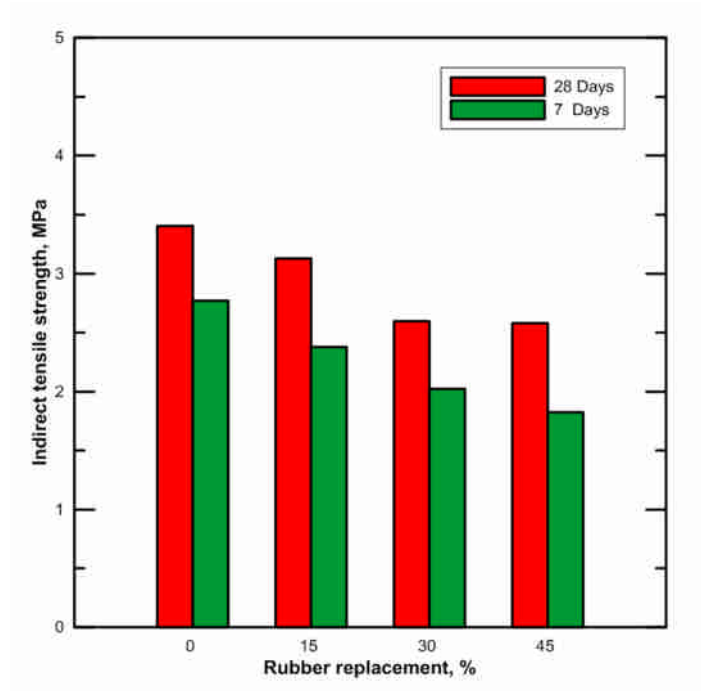


Figure 5: Indirect tensile strength for examined mixtures

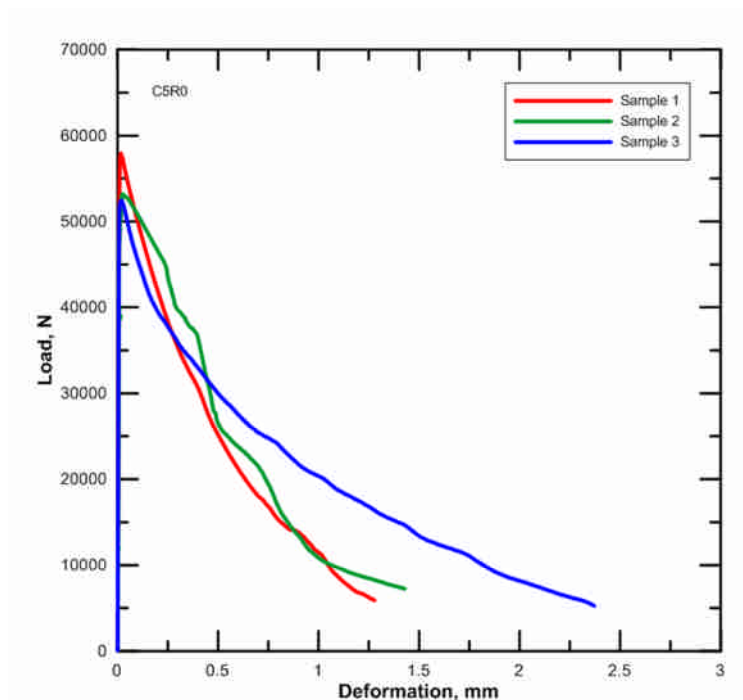


Figure 6: for different replacement levels: a. C5R0; b.C5R15; c. C5R30; and d. C5R45

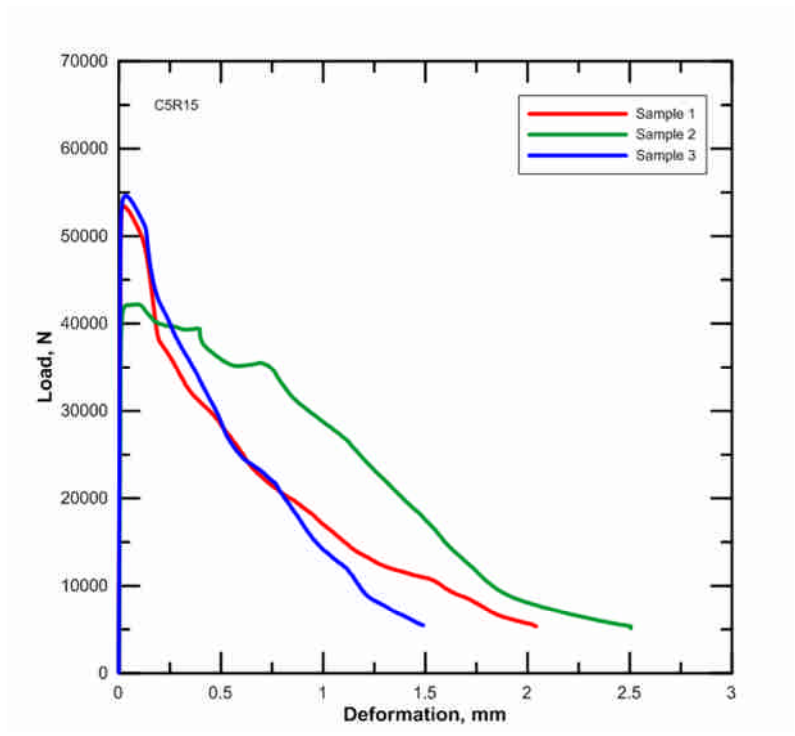


Figure 6: b

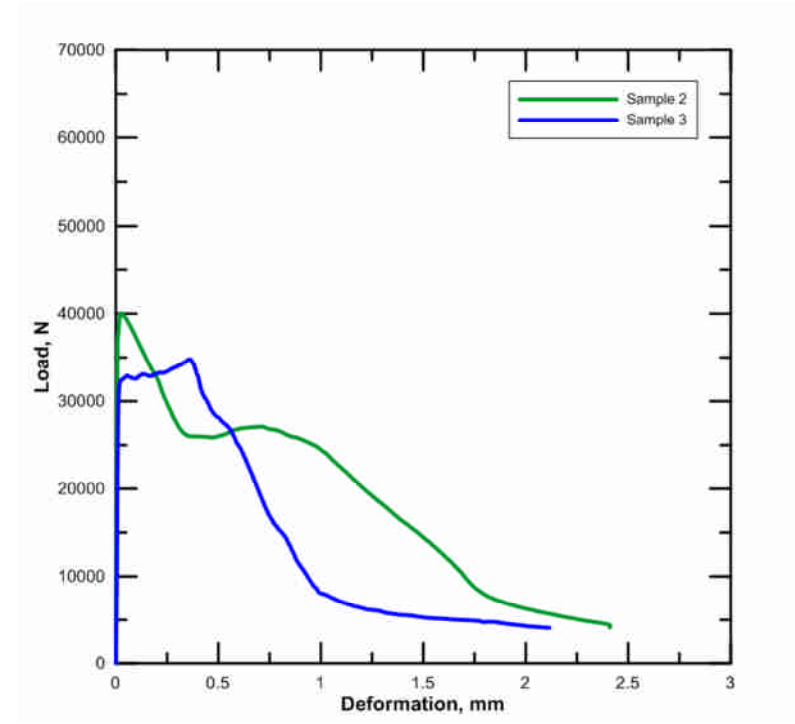


Figure 6: c

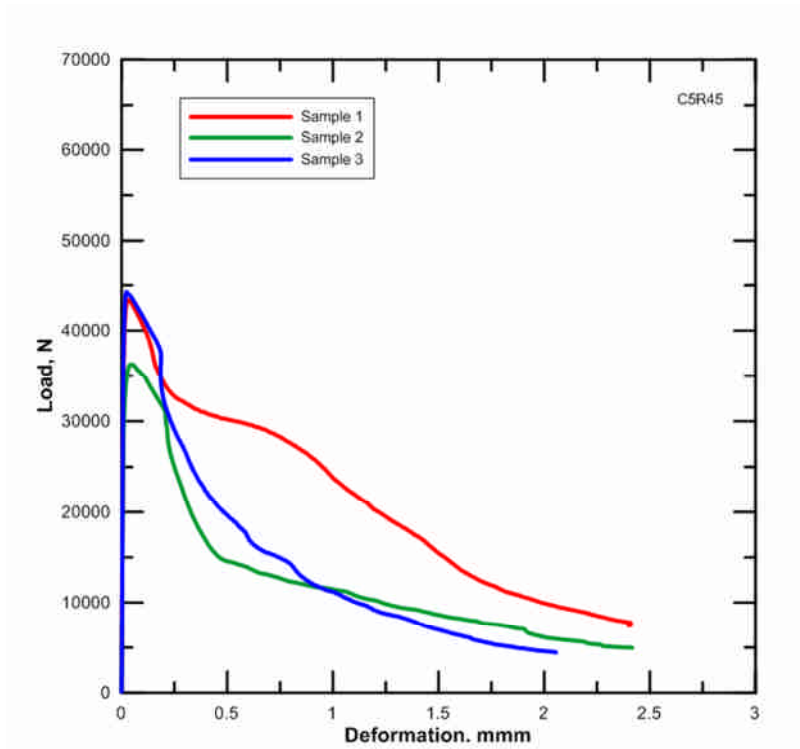


Figure 6: d

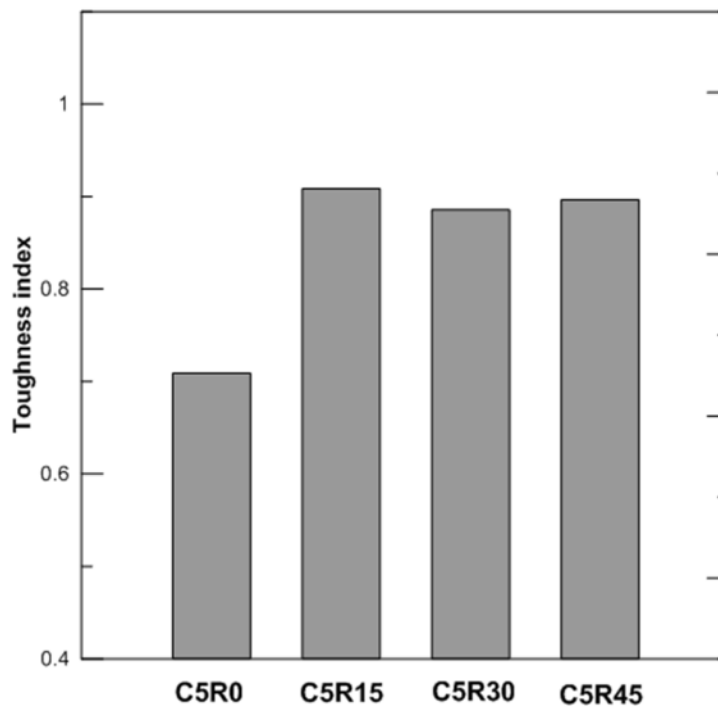


Figure 7: Effect of replacement on toughness indices.

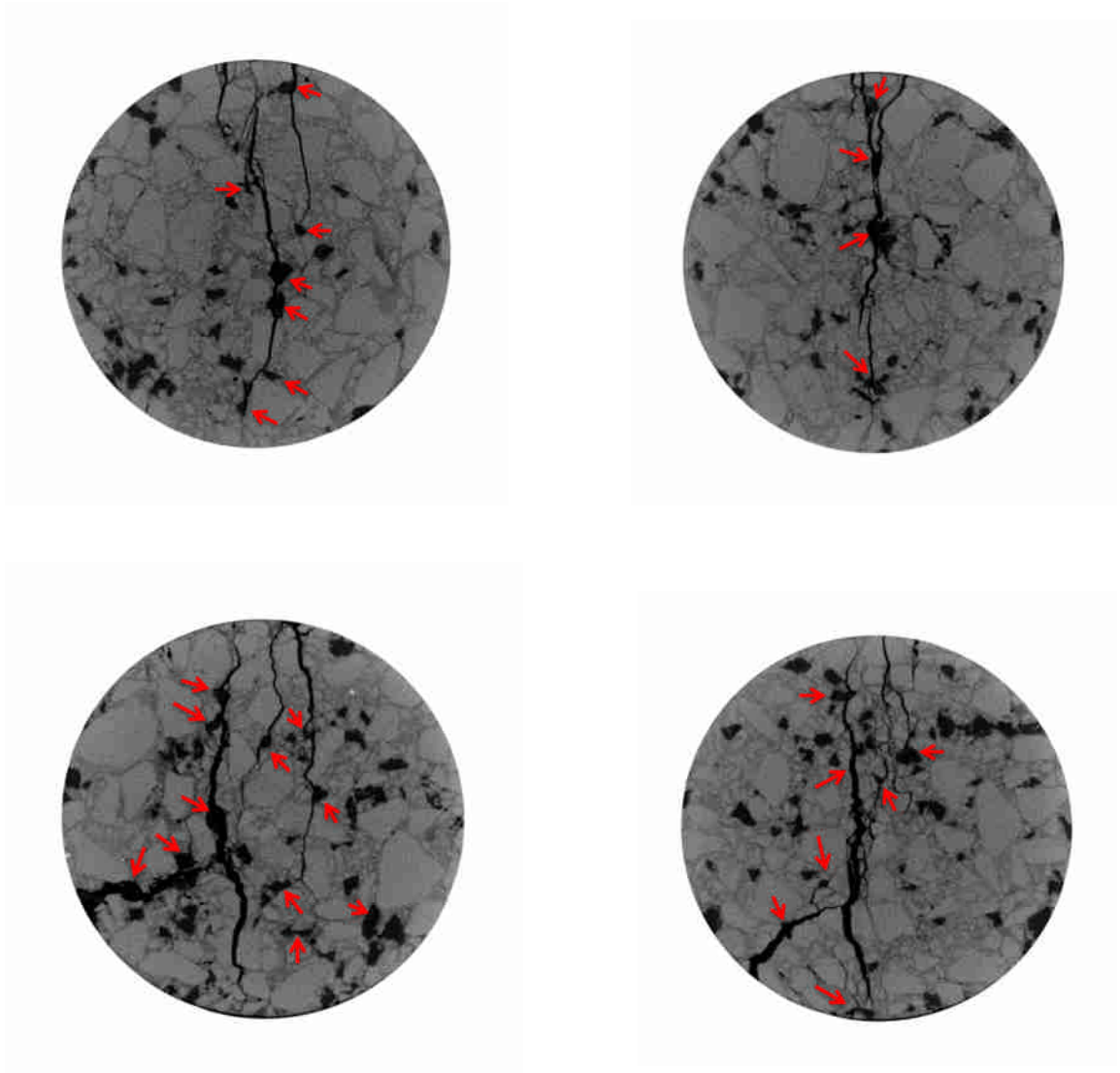


Figure 8: Sample scans of the failed specimens showing crack propagation through rubber particles: A and B represents the mixtures with 30% and 45% rubber replacement, respectively.

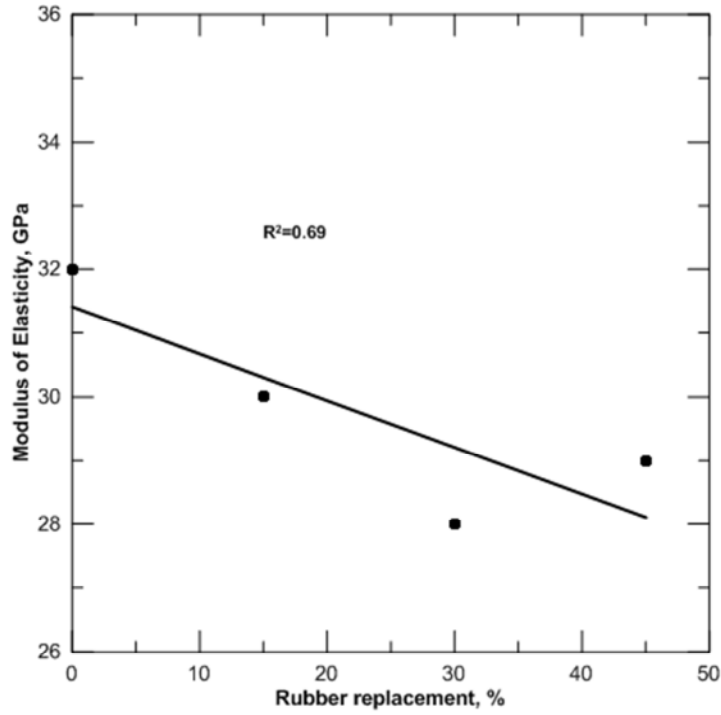


Figure 9: Effect of rubber content on static modulus of elasticity.

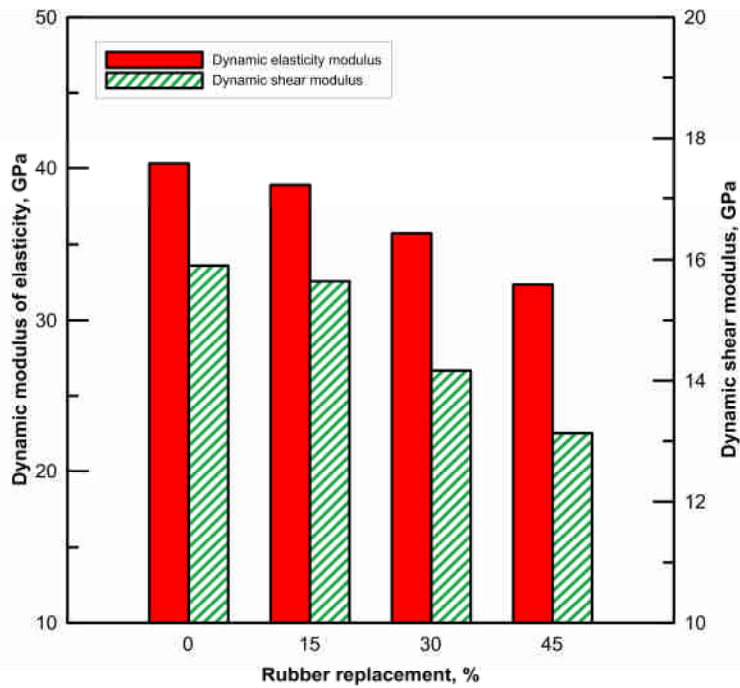


Figure 10: Effect of rubber replacement on dynamic elasticity and shear moduli

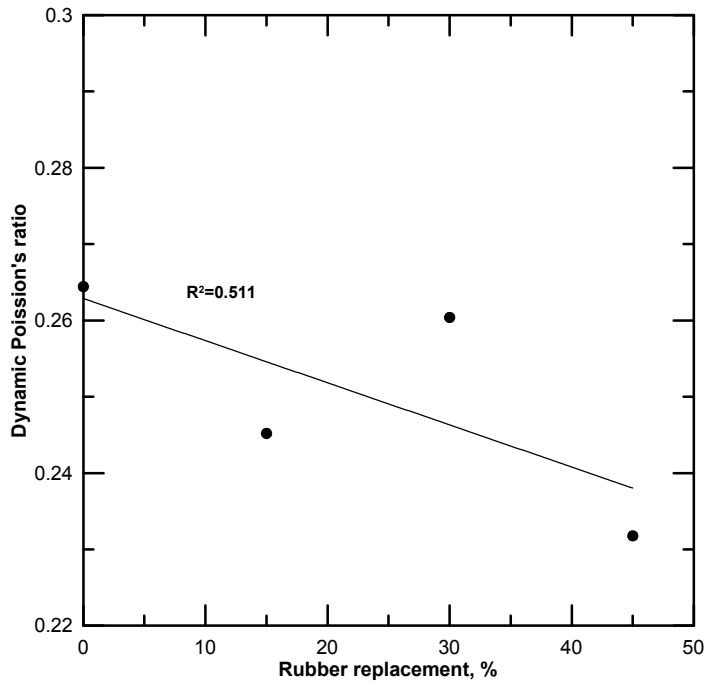


Figure 11: Effect of rubber replacement on dynamic Poisson's ratio

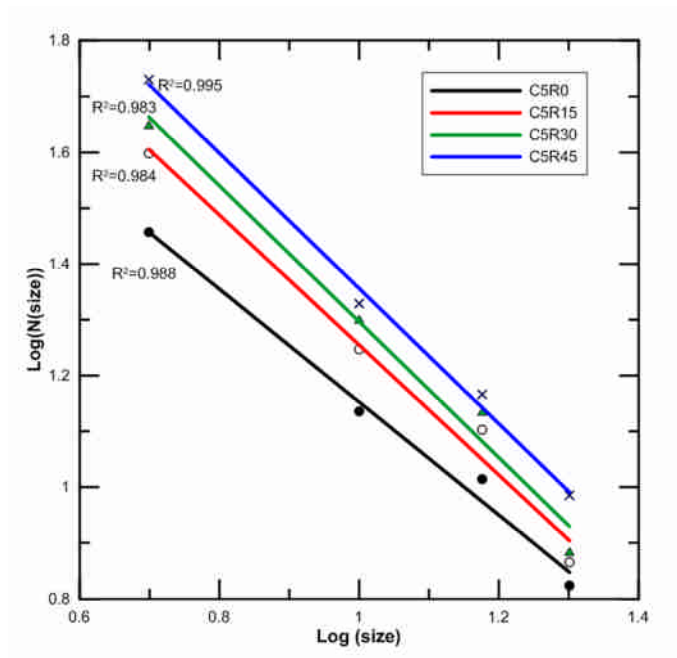


Figure 12: Fractal dimensions for virgin and modified mixtures with different replacement level



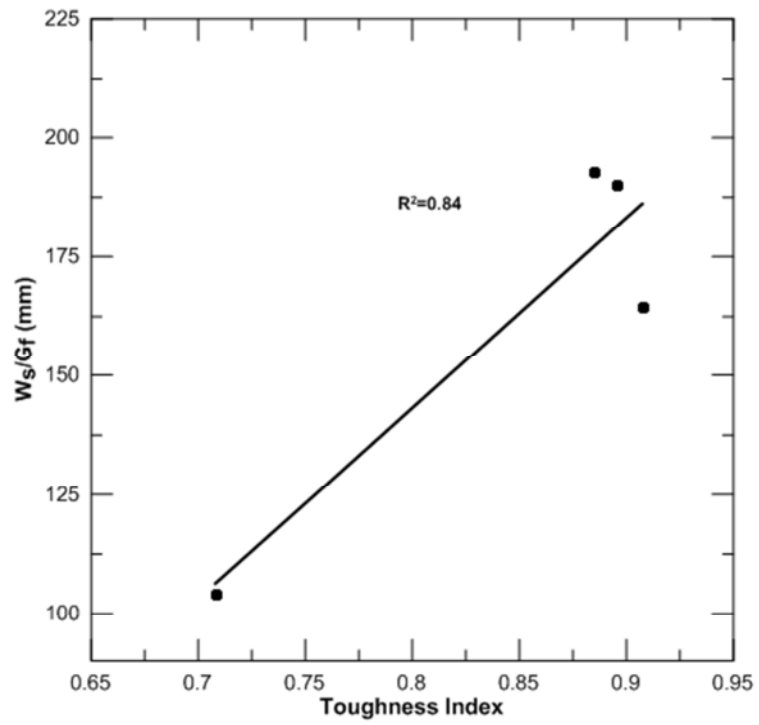


Figure 13: Correlation between mechanical and fractal analysis results